A novel WFS technique for high-contrast imaging: Phase Sorting Interferometry (PSI)

Johanan L. Codona, Matthew A. Kenworthy, and Michael Lloyd-Hart

Steward Observatory, University of Arizona, Tucson, AZ 85721

ABSTRACT

High-contrast adaptive optics (AO) observations near stars have to contend with the telescope's diffraction halo, a rapidly-changing cloud of residual atmospheric speckles, and a host of faint but persistent quasi-static speckles caused by various imperfections and aberrations. It is these quasi-static speckles that typically limit the detection sensitivity near stars as they are easily confused with faint stellar companions. Since they are coherent with the starlight, it is possible to suppress the quasi-static speckles and other residual diffraction halo over a search region by applying small offsets to the AO system's deformable mirror (DM). Computing the required offsets requires knowledge of the location, brightness, and phase of the speckle relative to the star's PSF core.

We present a new wavefront sensing technique for measuring the static halo that uses the randomly-changing residual AO speckles as interferometric probes. Doing this requires simultaneous short-exposure frames from a mid-IR science camera and measurements of the residual closed-loop wavefront using the AO system's wavefront sensor (WFS). These data streams are combined to construct a map of the quasi-static halo's complex amplitude near the bright core of a star's PSF, permitting its adaptive suppression. Implementing this new WFS and halo-suppression servo requires no new hardware, just new processing applied to the existing AO system. By suppressing the quasi-static speckles, we are left with only the fast speckle noise, which should average to a smooth background.

Keywords: Extreme adaptive optics, high-contrast imaging, focal-plane interferometry,speckle suppression.

1. INTRODUCTION

At the University of Arizona, we are developing a new technique for suppressing the diffraction halo called "phase apodization coronagraphy" (PAC).[1] Such suppression is needed for high-contrast imaging in the mid and longer infrared wavelengths because the high Strehl delivered by the AO system makes the diffraction pattern the constraining factor limiting sensitivity close to the star. The diffraction halo suppression is accomplished using an apodizing phase plate (APP)[2,3] placed in a pupil of the Clio[4] mid-IR imager. Unlike conventional coronagraphs that work by arranging an artificial eclipse with a transmission or phase mask in the focal plane, followed by a Lyot stop to trim the starlight diffracted by the focal plane stop, the PAC uses a single pupil optic (Figure 1). It works by intentionally diffracting starlight into a halo with equal amplitude and opposite phase to the diffraction pattern over a specified region of the focal plane. Since the halo symmetries of a pupil diffraction pattern and that of a phase mask differ, the diffraction suppression can only be carried out over half the field of view around the star at a time. Since the APP is a pupil optic, the PAC technique does not require the careful aiming that is a feature of Lyot coronagraphs, but works over the entire field of view. With the periodic nodding required for IR observing, this buys back at least a factor of two in efficiency over a focal plane mask system. Another PAC advantage is that it largely retains the full resolution of the telescope, and works well with arbitrary (e.g. segmented) apertures.

Depending on the science objectives, an aggressive goal for ground-based observations is 5-6 decades fainter than the star at 2-3 λ/D. For reference, the Airy pattern is ~ 2 decades fainter than the star at this radius, and rapidly-changing uncorrected atmospheric speckles left over by the AO system in the mid-IR are perhaps 3 decades fainter than the star. The speckles have timescales that depend on the processing characteristics of the AO system, the projected wind velocity in the focal plane, and the location of the speckles relative to the star. In general, processing-lag dominated residual AO speckles have longer timescales nearer to the star, and can live

Adaptive Optics Systems, edited by Norbert Hubin, Claire E. Max, Peter L. Wizinowich,
Proc. of SPIE Vol. 7015, 70155D, (2008)
0277-786X/08/$18 · doi: 10.1117/12.790024

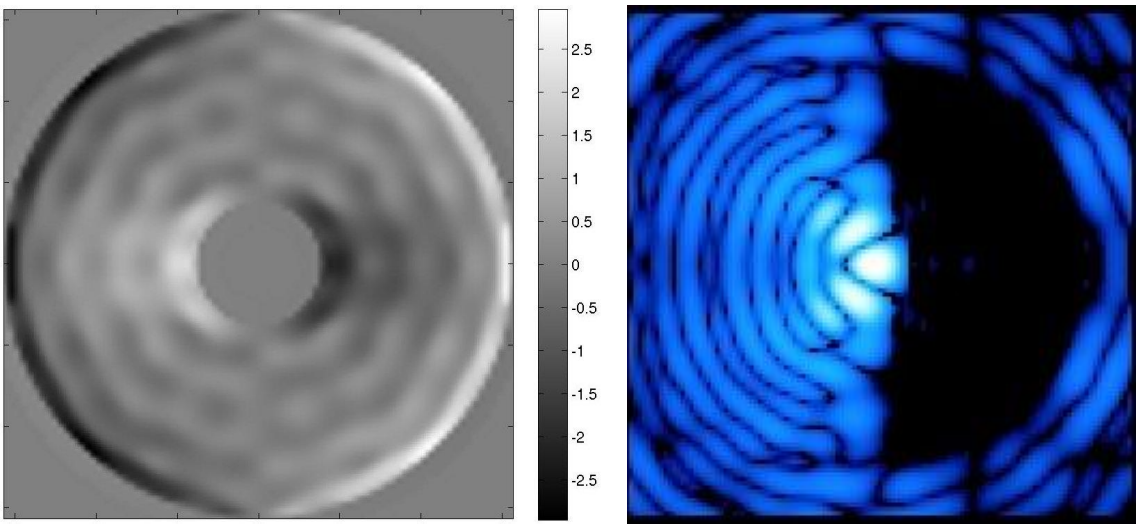

(a) Phase mask design for an MMT PAC APP.

(b) Ideal PSF corresponding to the APP in (a). The log intensity scale is 5 decades normalized to the peak of the star.

Figure 1. Phase Apodization Coronagraph (PAC) for the MMT. By placing an apodizing phase plate (APP) into a reimaged pupil, all stars in the field will appear with dark D-shaped regions in their PSFs. The design shown here has a 50% Strehl ratio, suppresses inward to the first Airy ring, and outward to $8\lambda/D$, which is comparable with the MMT's AO control radius. The PSF is shown with a 5 decade log scale, which is appropriate for the fast speckle noise in a 4 hour exposure. In reality, the image would have quasi-static speckles from about 3 decades and fainter than the star, obscuring the view of faint stellar companions.

for tens to hundreds of milliseconds depending on circumstances. This speckle timescale governs the incoherent $1/\sqrt{T}$ speckle-averaging process that reduces the speckle σ another 2-3 decades over a night's exposure. This speckle averaging process is well-known to be stopped by the ubiquitous presence of faint but nearly static speckles caused by aberrations within the optical system itself. These speckles do change, slowly, but not fast enough to average, nor are they repeatable enough to be calibrated. They can, however, be compensated for at observation time by "dialing-in" appropriate anti-speckle ripples with the deformable mirror (DM),[1,5] but the information required to do so must be acquired during the observation. A faint speckle of size λ/D can be suppressed by applying a small sinusoidal ripple across the DM with a wavevector equal to $k\theta$, an amplitude measured in wavefront phase equal to the square root of the contrast between the speckle and the star, and a phase relative to the pupil that is determined from the phase of the speckle light relative to the star's diffraction-limited core.

Codona and Angel[1] described a closed-loop halo suppression algorithm based on measurements made with a coronagraphic focal plane interferometer (CFPI). A closed-loop laboratory demonstration of this concept was built by Codona with graduate student Nicole Putnam.[6] The algorithm worked robustly and in a few cycles converged on DM shapes that nulled out pure or phase-distorted diffraction rings, even with errors of ~ 1 radian in the phase measurement. The closed-loop algorithm did not rely on using the CFPI method to measure the residual halo phase, and any other method that provides equivalent information could be substituted. Since the halo suppression servo proved to be so robust to measurement noise, it makes sense to use it at the telescope to suppress the semi-static speckles that limit detection. In this paper, we describe a new concept for measuring the static speckles and residual diffraction pattern of an AO-corrected halo, with the ultimate goal of suppressing it.

In the next section, we consider our options for measuring the quasi-static speckles and other residual diffraction halo artifacts in the presence of fast residual AO speckles. We then introduce a new approach that uses the residual AO speckles themselves as interferometric probes of the halo. Finally, we carry out a proof of concept simulation and show that it does indeed allow us to estimate the underlying static halo.

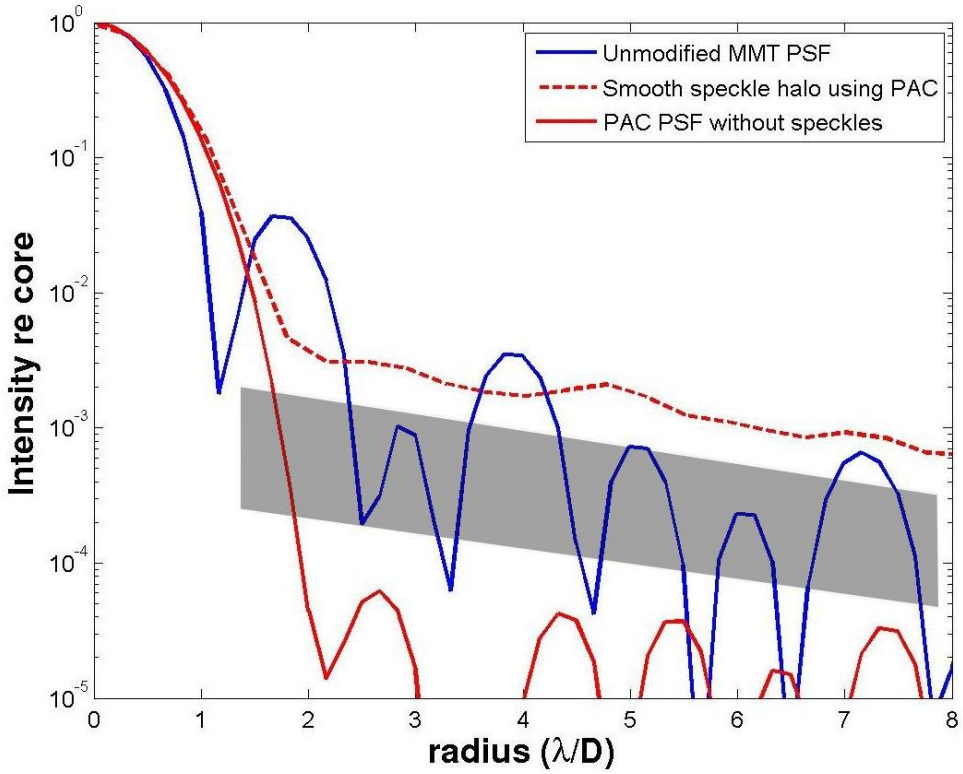

Figure 2. Radial cuts through the unmodified MMT PSF (blue), the MMT/PAC PSF if there were no speckles (solid red), and with the smooth residual speckle halo (dashed red). The gray zone indicates where slow/semi-static "super-speckles" begin to appear. New semi-static speckles are expected at all fainter levels.

2. OPTIONS FOR MEASURING THE COMPLEX HALO

Residual halo suppression requires first detecting the undesired speckles and then measuring their location, amplitude, and phase. Detection of these speckles is aided by the PAC halo suppression, but it is not essential to our goal. The idealized situation is a faint speckle, 3 or more decades fainter than the star in a region of the focal plane that has a suppressed (or otherwise negligible) diffraction halo, in the presence of rapidly-changing bright residual AO speckles. Any methods that use images near the pupil plane will have to contend with the known but complicated PAC phase pattern, as well as being susceptible to non-common-path errors. If the diffraction halo is bright enough under the speckle and has a well-modeled phase variation with focus, a defocus-based approach might be applied. However, defocus immediately decreases the intensity of the speckle, making the faintest speckles disappear before they can be measured.

A coronagraphic focal plane interferometer (CFPI)[1,6,7] would work, so long as the corrected Strehl ratio is high enough to provide a reasonable interferometric reference beam. CFPI uses a small reflecting focal plane mask to access the phase reference starlight, with or without a Lyot stop. This requires the complexity and cost of extra optical hardware, and inherits the careful guiding requirements of the Lyot coronagraph, which are exacerbated by the constant nodding for infrared sky background subtraction. In a stable low-background situation like a space telescope, the CFPI would be a much more attractive choice.

The technique we loosely call here "speckle steering" uses the AO system's DM to create a wavefront ripple, introducing a controlled speckle at the desired focal plane location, with a controlled phase and amplitude.[8] By changing the phase of the ripple and hence the speckle, the intensity of the coherent sum of the speckle and the subject halo feature modulate, with the maximum intensity occuring when the speckle and halo phases coincide. In a much more sophisticated treatment,[9] this was used with the JPL HCIT experiment to drive the residual halo of the coronagraph down to TPF levels.[10] While this was a remarkable achievement, it did not have to contend

with a cloud of rapidly changing residual AO speckles only 2–3 decades fainter than the star, which, although instantaneously coherent, act like a bright incoherent background in longer exposures. To perform a similar analysis in a reasonable amount of time using the AO DM on a ground-based telescope, the probe speckles would have to be brighter than the AO speckles. In that limit the measurement accuracy of underlying halo would asymptotically depend on it's own photon flux, making it possible to measure and suppress the faint residual static halo structure in the presence of much brighter residual AO speckles. However, this has the cost of having to introduce a bright probe speckle—indeed an array of them, which will negatively impact sensitivity more than the improvement of having suppressed the original faint static speckles. This problem can be aleviated by multiplexing science and WFS frames, but the loss of integration time will also incur a significant loss of sensitivity over a fixed exposure. Also, using the same DM to make the subtle wavefront corrections to suppress the static speckles and then using it to create the bright probe speckles introduces issues of repeatability and stability. These problems would be moot if we were to just use the DM to correct the field and not also to probe it.

3. A NEW TECHNIQUE: PHASE SORTING INTERFEROMETRY

While contemplating an effective static speckle WFS approach for the MMT with the lowest cost of implementation, we were inevitably drawn to the speckle steering approach. While discussing the downside of the bright speckle probe halo, coauthor Michael Lloyd-Hart first suggested that we consider using the unavoidable speckle field left by the AO system. The residual speckle halo is beyond the control of the AO system due to a combination of fitting and processing lag errors, as well as WFS shot noise and other causes. This does not mean that we do not have a reasonable knowledge of the residual wavefront errors. The AO WFS provides us with a high-speed view of the residual deviations of the wavefront. At the MMT, the natural guide star Shack-Hartmann WFS operates in visible red, while the Clio camera[4] is currently being carried being used for self-luminous exoplanet surveys in the M band ($\sim 4.8\,\mu$m). The rms phase residuals in M band are about $1/3$ radian, which are small enough to be reasonably analyzed using a linear Taylor expansion. Using Fourier optics, if the static focal plane field (including all effectively static features) is $\widetilde{\psi}_0(\kappa)$ where $\kappa = k\boldsymbol{\theta}$ is the spatial frequency wavevector, $\boldsymbol{\theta}$ is the angle away from the star, and the PSF is $\Phi(\boldsymbol{\kappa}) = \left|\widetilde{\psi}(\boldsymbol{\kappa})\right|^2$, the speckle field caused by the small residual wavefront errors (residual phase:$\phi(\mathbf{x})$) is $\delta\widetilde{\psi}(\kappa) \approx i\widetilde{\psi}_0 * \widetilde{\phi}$. This means that realizations of the weak speckle field are composed of diffraction-limited speckles with anti-Hermitian symmetry across the star. The speckle field itself does not have enhanced power near Airy rings or other structures, but has a mean distribution determined by the statistics of the random wavefront and the various spatial and temporal properties of the AO system as well as the turbulence and the wind. Wind advection couples with the AO servo to leave speckles preferentially distributed in the direction of the wind vector projected onto the sky. These lag error speckles evolve more slowly than seeing-limited speckles, with longer timescales closer to the star.[7] This is caused by a repeating servo correction error as the AO system chases the wind-driven wavefront aberrations across the pupil.

These unwanted speckles have ideal halo probing properties in that they become brighter and slower nearer to the star, are already measured as a matter of course by the AO WFS in exactly the manner required to use them as probes, and do not require adding any other light to the halo or diagnostic tuning of the DM. A large sinusoidal phase ripple with N crest-to-crest spatial periods per aperture diameter D and an advection speed perpendicular to the crests of $v_\perp$ will cause speckles with slowly changing intensity but constantly changing phase and a 2π period of $T = D/Nv_\perp$. With a fast frame rate camera, a speckle sitting on the static halo will coherently interfere, exhibiting a sinusoidal variation in intensity with period T. The radii of greatest astronomical interest are the closest possible using our PAC technique, which are as small as 1.5–2 λ/D. Depending on the wind speed, the speckle phase-wrapping timescale at these radii can be well over 100 ms, with smaller values farther out and in stronger winds. In comparison, the WFS frame rate at the MMT is faster than 500 fps, providing a high temporal resolution view of the residual wavefront, and by Fourier transform, the evolving speckles' complex amplitude. Speckle images taken with longer frame rates will suffer reduced contrast and aliasing, but with proper synchronization the high WFS frame rate should still allow interpretation. Normally, the fast speckle's amplitude and phase changes randomly along with the wind-driven phase wrapping, requiring a statistical analysis. Again, the WFS data is sufficient to not only estimate speckle phase and intensity, but to collect and constantly update field statistics that might otherwise bias the analysis. We will limit our discussion

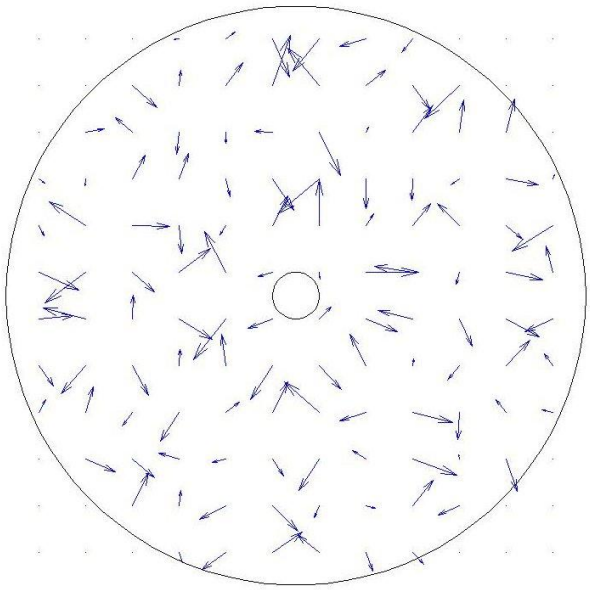

Figure 3. Residual WFS data in closed-loop gives the wavefront slopes at a grid of 12 x 12 points across the aperture at 527 Hz.

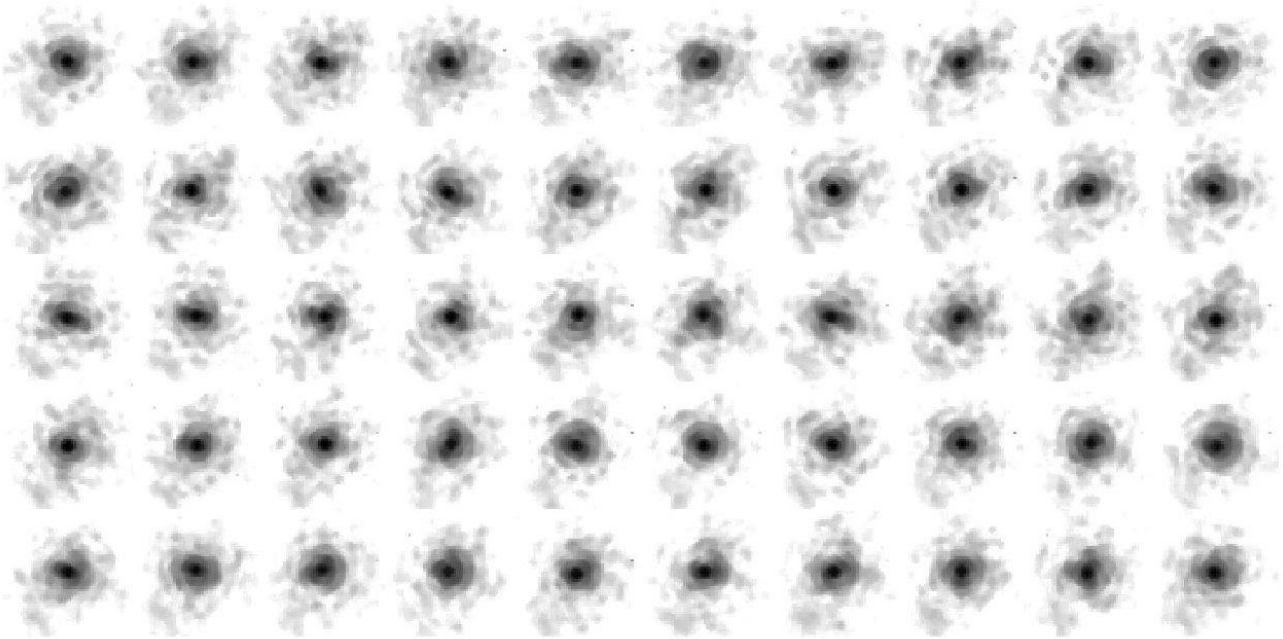

Figure 4. Consecutive 15 FPS Clio frames of a bright star showing changing speckles and Airy pattern. While the temporal evolution of the speckles is not well resolved at this frame rate, there are still well-defined changing speckles that can be used with the integrated WFS information to probe the halo.

here to the relatively uncomplicated case of a cloud of residual AO speckles resulting from boiling turbulence corrected with fitting and lag error.

Phase-Sorting Algorithm

The WFS measurements, along with the fastest practical frame rate images from the science camera, provide the two data sets from which we can derive the complex static halo. First, for every WFS slope measurement, we use the AO system's reconstructor to estimate the residual wavefront, $z(\mathbf{x})$, and hence the wavefront phase at the science wavelength, $\phi(\mathbf{x}) = 2\pi z(\mathbf{x})/\lambda_{science}$. Masking this phase map with a pupil and Fourier transforming (times i) allows us to compute the residual speckle field at the WFS frame rate. By integrating the *complex* speckle field down to a rate commensurate with the science camera images, we can compute a corresponding residual phase and amplitude map, as well as making estimates of the speckle-halo partial coherence after integration. For determining the phase of the static halo, only the residual phase of the integrated fast speckle map is required. We next create a *minimum of 3* phase-sorted science camera and count frames, which will be populated from the science camera images keyed by the computed complex speckle frames. For simplicity and familiarity, we will use 4 phase-sorting bins, centered on $\{0, \pi/2, \pi, 3\pi/2\}$, each $\pm\pi/4$ in phase. We refer to the pixels of the science frame as $I(t)$ and the corresponding phase map of the integrated residual speckles derived from the WFS measurements as $\varphi(t)$. The phase-sorted images are labelled $\mathcal{I}_0$, $\mathcal{I}_{90}$, $\mathcal{I}_{180}$, and $\mathcal{I}_{270}$ and the count images are $\mathcal{N}_0$, $\mathcal{N}_{90}$, $\mathcal{N}_{180}$, and $\mathcal{N}_{270}$. All 8 images are initialized to zero at the start of an integration.

For each frame from the science camera (after appropriate cleaning and centering, etc.), we take each pixel and add it to the corresponding phase-binned image according to the phase of the corresponding pixel of the integrated phase map. At the same time, we also *increment* the corresponding pixel of the phase-binned count image each time we add to a pixel. After integrating long enough to reasonably populate all of the pixels in the sorted images, we can estimate a complex image

$$\xi = \left(\frac{\mathcal{I}_0}{\mathcal{N}_0} - \frac{\mathcal{I}_{90}}{\mathcal{N}_{90}}\right) + \left(\frac{\mathcal{I}_{180}}{\mathcal{N}_{180}} - \frac{\mathcal{I}_{270}}{\mathcal{N}_{270}}\right) i$$

the phase of which gives the phase of the underlying halo, and the amplitude gives the rms amplitude of the partially-coherent portion of the speckle halo after integration times the amplitude of the underlying static halo. Since the WFS measurements allow us to collect all of the speckle statistics required to also estimate the static halo amplitude, the phase sorting method gives us all of the information required to adjust the DM to further suppress the halo. A continuing cycle of measurements and corrections will track the quasi-static speckles as they change, with fainter speckles being measured and suppressed as the science exposure continues.

4. NUMERICAL SIMULATION OF PHASE SORTING INTERFEROMETRY

To validate the PSI concept, we modeled the MMT AO system including a PAC APP, and used the residual wavefront phase with a 4-bin PSI algorithm to recover the static halo phase. The atmospheric wavefront was modeled with properties typical of those measured at the MMT (r_0 = 15 cm @ 500 nm, outer scale L_0 = 30 m, τ_0 = 3 ms at 500 nm). "Boiling" turbulence was simulated by superposing three wind layers with randomly dithered velocities around 20 m/s and wind directions dithered near 0° and ±45°. The wavefront as corrected by the MMT AO system was modeled by first applying a low-pass spatial filter to model the fitting error corresponding to 56 corrected modes, and the temporal servo lag was modeled by subtracting the current unsmoothed wavefront from the smoothed wavefront from 7 ms earlier. The choice of 7 ms lag was selected to give the observed M-band Strehl ratio of 90%. A total of 8 seconds of wavefronts and intensity images were computed at 1 kHz and then integrated down to more realistic frame rates. The accuracy of the simulated results was checked by comparing integrated simulation frames with actual Clio frames of bright stars (e.g. figure 4), looking for reasonable speckle amplitudes, angular power distribution, and time scales. The 1 ms simulated complex amplitude frames were averaged over 33 ms, 100 ms, and 179 ms (a Clio frame rate) and compared in figure 5 to show the effect of slower science camera frame rates in smoothing out the usable probe speckles. For the modeled parameters, a frame rate of 15 FPS or greater should be adequate to probe within 5–8 λ/D. Faster frame rates are better as they directly increase the effective partial coherence. We used 30 FPS as the science camera frame rate.

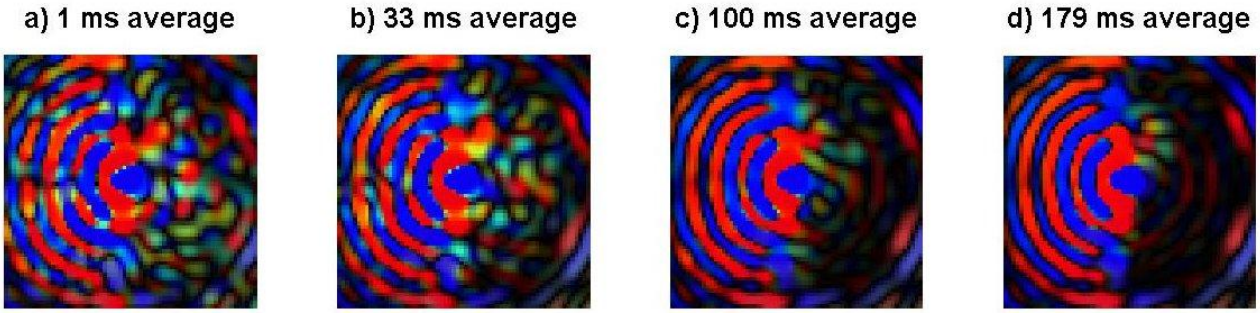

Figure 5. This figure shows the effect of exposure integration on the complex halo. The diffraction halo is syeady and unaffected, but the complex speckles wander and average to zero. Since the complex evolution of lag error speckles is slower nearer the star, the averaging is non-uniform. In the PSI algorithm, only the speckle portion of the integrated complex halo would be used for phase sorting the science images.

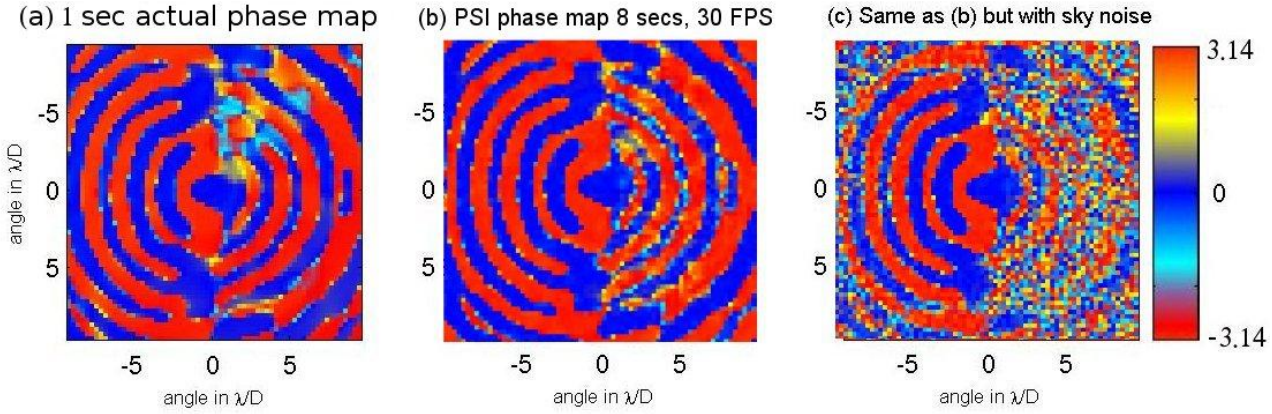

Figure 6. Complex halo phase recovery using the PSI algorithm with 8 seconds of simulated 30 FPS M-band data phase-sorted using simulated residual wavefronts as would be obtained from the Shack Hartmann wavefront sensor. (a) true phase averaged for the 8 secs at 1 ms sampling rate. (b) PSI recovered phase with no sky noise. (c) same as (b) but with realistic levels of sky noise added. Phase is encoded by color as indicated, with no intensity modulation.

The simulated 30 FPS PSF images were phase-sorted into 4 phase bins according to the phase of the computed complex speckle field, integrated to the same 30 FPS frame rate. Sky and readout noise appropriate for the 33 ms integrations were added to each PSF image prior to phase sorting. Following the PSI algorithm, the static halo phase was computed (figure 6) and should be compared with the phase from the averaged halo in figure 5. Due to the small amount of time in the simulation, the complex speckles very near the star have yet to fully average out and are still biasing the result, an effect which can actually be seen in the PSI estimate as well. The simulation is mostly a qualitative proof of concept, but it shows that even in a few seconds of processing, PSI is beginning to show the presence and phase of the residual diffraction rings within the dark D. This phase alternates by π radians between rings, the same as for an un-apodized Airy pattern. The recovered phase in the center and right hand panels is noisy but clearly detectable, with an rms error in 1 sec of ~ 1 radian.

5. CONCLUSIONS

Phase-sorting interferometry appears to provide a practical new technique for measuring the quasi-static speckles that limit detection of faint objects such as exoplanets very near stars. The technique uses the rapidly-changing residual speckles left by the AO system to probe the static portion of the halo but adds no other diagnostic light to the halo. By themselves, the residual AO speckles would normally not be useful, but by also making use of the AO system's closed-loop residual WFS measurements, we are able to compute the phase of the fast

speckles and use that information to analyze the intensity fluctuations seen in the science camera frames. This is done by phase-sorting the science camera pixels into a form that can be processed as with a more conventional phase-stepping interferometer to give an estimate of the complex static halo. This information can then be used to drive a halo-suppression algorithm using subtle offsets to the DM (or, more indirectly, by offsets to the WFS). Without the quasi-static speckles, the sensitivity of a long exposure would ultimately be set by the smoothly-averaging residual AO speckles which should allow a 5 sigma 5 decade detection in a single night. A simple simulation of the AO system operation confirms the feasibility of this method, which can be implemented with virtually no new hardware at the telescope save for a computer to capture and process the data. The next step is to verify the ability to use the residual speckles and WFS data at the telescope to actually measure the complex halo of a bright star.

6. ACKNOWLEDGMENTS

We would like to thank Roger Angel for his support and assistance during the genesis of this project.

REFERENCES

1. J. L. Codona and R. Angel, "Imaging Extrasolar Planets by Stellar Halo Suppression in Separately Corrected Color Bands," ApJ **604**, pp. L117–L120, Apr. 2004.
2. J. L. Codona, M. A. Kenworthy, P. M. Hinz, J. R. P. Angel, and N. J. Woolf, "A high-contrast coronagraph for the MMT using phase apodization: design and observations at 5 microns and 2 λ/D radius," in *Ground-based and Airborne Instrumentation for Astronomy. Edited by McLean, Ian S.; Iye, Masanori. Proceedings of the SPIE, Volume 6269, pp. 62691N (2006).*, *Presented at the Society of Photo-Optical Instrumentation Engineers (SPIE) Conference* **6269**, July 2006.
3. M. A. Kenworthy, J. L. Codona, P. M. Hinz, J. R. P. Angel, A. Heinze, and S. Sivanandam, "First On-Sky High-Contrast Imaging with an Apodizing Phase Plate," ApJ **660**, pp. 762–769, May 2007.
4. S. Sivanandam, P. M. Hinz, A. N. Heinze, M. Freed, and A. H. Breuninger, "Clio: a 3-5 micron AO planet-finding camera," in *Ground-based and Airborne Instrumentation for Astronomy. Edited by McLean, Ian S.; Iye, Masanori. Proceedings of the SPIE, Volume 6269, pp. 62690U (2006).*, *Presented at the Society of Photo-Optical Instrumentation Engineers (SPIE) Conference* **6269**, July 2006.
5. F. Malbet, J. W. Yu, and M. Shao, "High-Dynamic-Range Imaging Using a Deformable Mirror for Space Coronography," PASP **107**, pp. 386–+, Apr. 1995.
6. N. Putnam, J. L. Codona, and J. R. P. Angel, "Laboratory demonstration of a focal plane coronagraphic interferometer designed for anti-halo apodization of starlight," in *Advances in Adaptive Optics II. Edited by Ellerbroek, Brent L.; Bonaccini Calia, Domenico. Proceedings of the SPIE, Volume 6272, pp. 62722M (2006).*, *Presented at the Society of Photo-Optical Instrumentation Engineers (SPIE) Conference* **6272**, July 2006.
7. R. Angel, "Imaging Extrasolar Planets from the Ground," in *ASP Conf. Ser. 294: Scientific Frontiers in Research on Extrasolar Planets*, pp. 543–556, 2003.
8. M. A. Kenworthy, P. M. Hinz, J. R. P. Angel, A. N. Heinze, and S. Sivanandam, "Whack-a-speckle: focal plane wavefront sensing in theory and practice with a deformable secondary mirror and 5-micron camera," in *Advances in Adaptive Optics II. Edited by Ellerbroek, Brent L.; Bonaccini Calia, Domenico. Proceedings of the SPIE, Volume 6272, pp. 62723B (2006).*, *Presented at the Society of Photo-Optical Instrumentation Engineers (SPIE) Conference* **6272**, July 2006.
9. P. J. Bordé and W. A. Traub, "High-Contrast Imaging from Space: Speckle Nulling in a Low-Aberration Regime," ApJ **638**, pp. 488–498, Feb. 2006.
10. J. T. Trauger and W. A. Traub, "A laboratory demonstration of the capability to image an Earth-like extrasolar planet.," *Nature* **446**, pp. 771–773, Apr. 2007.